



UNIVERSITY OF LEEDS

This is a repository copy of *Role of Bacterial Cell Surface Sulfhydryl Sites in Cadmium Detoxification by Pseudomonas putida*.

White Rose Research Online URL for this paper:
<http://eprints.whiterose.ac.uk/156572/>

Version: Accepted Version

Article:

Yu, Q, Mishra, B and Fein, JB (2020) Role of Bacterial Cell Surface Sulfhydryl Sites in Cadmium Detoxification by *Pseudomonas putida*. *Journal of Hazardous Materials*, 391. 122209. ISSN 0304-3894

<https://doi.org/10.1016/j.jhazmat.2020.122209>

© 2020, published by Elsevier. This manuscript version is made available under the CC-BY-NC-ND 4.0 license <http://creativecommons.org/licenses/by-nc-nd/4.0/>.

Reuse

This article is distributed under the terms of the Creative Commons Attribution-NonCommercial-NoDerivs (CC BY-NC-ND) licence. This licence only allows you to download this work and share it with others as long as you credit the authors, but you can't change the article in any way or use it commercially. More information and the full terms of the licence here: <https://creativecommons.org/licenses/>

Takedown

If you consider content in White Rose Research Online to be in breach of UK law, please notify us by emailing eprints@whiterose.ac.uk including the URL of the record and the reason for the withdrawal request.



eprints@whiterose.ac.uk
<https://eprints.whiterose.ac.uk/>

**Role of Bacterial Cell Surface Sulfhydryl Sites in Cadmium
Detoxification by *Pseudomonas putida***

Qiang Yu^{1,*}, Bhoopesh Mishra², Jeremy B. Fein¹

¹Department of Civil & Environmental Engineering & Earth Sciences, University of Notre Dame, Notre Dame, Indiana 46556, United States

² School of Chemical and Process Engineering, University of Leeds, Leeds LS29JT, United Kingdom

A revised manuscript submitted to *Journal of Hazardous Materials*

* Author for correspondence.

Tel: (574) 631-4534; Fax: (574) 631-9236; Email: qyu@nd.ed

1
2
3
4
5
6
7
8
9
10
11
12
13
14
15
16
17
18
19
20
21
22
23
24
25
26
27
28
29
30
31
32
33
34
35
36
37
38
39
40
41
42
43

Highlights

- *P. putida* detoxifies aqueous Cd using cell surface sulfhydryl sites.
- Cell surface sulfhydryl site concentrations vary as a function of growth time.
- Cell growth with Cd positively correlates to sulfhydryl site concentration.
- Cell growth with Cd is independent of the non-sulfhydryl site concentration.

44

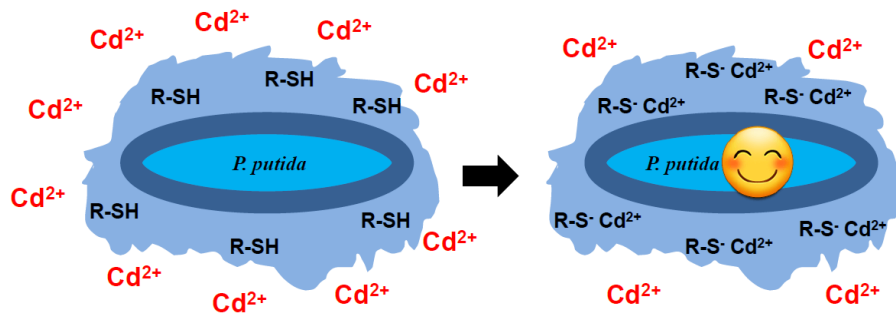
45

46

47

48

Graphical Abstract



49

50

51

52

53

54

55

56

57

58

59

60

61

62

Abstract

Understanding bacterial metal detoxification systems is crucial for determining the environmental impacts of metal pollution and for developing advanced bioremediation and water disinfection strategies. Here, we explore the role of cell surface sulfhydryl sites in bacterial detoxification of Cd, using *Pseudomonas putida* with surface sulfhydryl sites mostly on its EPS molecules as a model organism. Our results show that 5 and 20 ppm Cd in LB growth medium affects the lag phase of *P. putida*, but not the overall extent of cell growth at stationary phase, indicating that *P. putida* can detoxify Cd at these concentrations. EXAFS analysis of Cd bound to biomass from the different growth stages indicates that Cd binds to both sulfhydryl and non-sulfhydryl sites, but that the importance of Cd-sulfhydryl binding increases from early exponential to stationary phase. Cell growth is positively correlated to the measured sulfhydryl concentration on different biomass samples, but is independent of the measured non-sulfhydryl binding site concentration on the cell surfaces. Taken together, our results demonstrate that the sulfhydryl binding sites on EPS molecules can play an important role in binding and detoxifying toxic metals, significantly decreasing the bioavailability of the metal by sequestering it away from the bacterial cells.

86 **1. Introduction**

87 The presence of toxic metals in the environment, including both highly toxic metals (e.g., Hg
88 and Cd) and excess essential metals (e.g., Zn and Cu), can pose a severe threat to ecosystems.
89 Microorganisms, such as bacteria, can be sensitive to relatively low concentrations of toxic metals,
90 and they have developed multiple defense strategies to protect cells from toxic metals, such as cell
91 surface metal sequestration, metal efflux systems, intracellular metal sequestration, and metal
92 redox transformation (Gadd and Griffiths, 1978; Nies, 1999; Chandrangsu et al., 2017; Shou et al.,
93 2018). Understanding the metal detoxification systems of bacteria is crucial in order to determine
94 the environmental impacts of metal pollution on ecosystems and to develop appropriate strategies
95 for a variety of applications, such as bioremediation (Shamim, 2018; Liu et al., 2019), water
96 disinfection (Li et al., 2008), antimicrobial design (Turner, 2017), and biosynthesis of
97 nanomaterials (Wadhwani et al., 2016).

98 In most cases, metals must enter bacterial cells to cause toxic effects (Nies, 1999). Therefore,
99 blocking toxic metals before they cross cell membranes, e.g., immobilizing metals within the cell
100 envelope or on extracellular polymeric substances (EPS) (Gadd and Griffiths, 1978; Shou et al.,
101 2018) becomes an effective approach for lowering the bioavailability of toxic metals. Bacterial
102 cell envelopes and cell-bound EPS molecules (which together we refer to here as cell surfaces) can
103 adsorb a wide range of metals due to the presence of abundant functional groups (metal binding
104 sites) on molecules within cell surfaces, such as carboxyl, phosphoryl and sulfhydryl sites
105 (Beveridge and Murray, 1976; Liu and Fang, 2002; Fein et al., 2019). However, the toxicity and
106 bioavailability of the adsorbed metals on bacterial cell surfaces depends at least in part on the type
107 and concentration of the bacterial surface complexes that form (Flynn et al., 2014; Sheng and Fein,
108 2014). These results suggest that the type and location of binding sites that interact with aqueous

109 metals likely play an important role in regulating the toxicity of the adsorbed metals. To date, the
110 role of specific metal binding sites (e.g., carboxyl, phosphoryl and sulfhydryl sites) in the
111 detoxification of metals by bacteria has not been studied.

112 Compared to carboxyl and phosphoryl sites, sulfhydryl sites on bacterial cell surfaces are
113 generally less abundant (Yu et al., 2014), but they form much stronger bonds with chalcophile
114 metals such as Hg, Cd, Zn, Cu and Au (Yu and Fein, 2015; Nell and Fein, 2017; Yu and Fein,
115 2017b), resulting in the dominance of sulfhydryl sites in the adsorption of these metals onto
116 bacterial cells under low metal loading conditions (Guine et al., 2006; Mishra et al., 2010;
117 Pokrovsky et al., 2012; Yu and Fein, 2015). In addition, the concentration of sulfhydryl sites on
118 bacterial cell surfaces can increase significantly as a function of growth conditions (Yu and Fein,
119 2017a), and hence sulfhydryl sites can contribute significantly to the adsorption of Cd, Hg and Au
120 onto bacterial cells even under high metal loadings (Mishra et al., 2017; Yu and Fein, 2017b).
121 Therefore, we focus our study on sulfhydryl sites, and hypothesize that they play a crucial role in
122 sequestering toxic chalcophile metals on EPS molecules and away from the cell surface in order
123 to detoxify the metals. *Pseudomonas putida*, a bacterial species that can be found in many toxic
124 metal contaminated environments and exhibits excellent tolerance to chalcophile metals (Higham
125 et al., 1986; Chen et al., 2006; Hu and Zhao, 2007), was used as a model organism in our
126 experiments because under the growth conditions of our experiments it produces EPS molecules
127 that contain abundant sulfhydryl binding sites with much lower sulfhydryl site concentrations on
128 the cell walls. Therefore, *P. putida* is a prime candidate to exhibit EPS-dominated sulfhydryl
129 binding of metals and hence for use as a probe of the bacterial strategy of sequestering toxic metals
130 through EPS binding. Our results indicate that Cd adsorption onto EPS sulfhydryl sites represents
131 a strategy adopted by *P. putida* and perhaps other similar bacterial species for binding and

132 detoxifying Cd, and we demonstrate that the bioavailability, and hence the toxicity of Cd is
133 inversely related to the concentration of sulfhydryl sites within the cell-produced EPS molecules.

134

135 **2. Materials and Methods**

136 **2.1 Cd Toxicity Tests**

137 Two sets of toxicity tests were conducted using *Pseudomonas putida* (ATCC#: 33015) as
138 the model organism, and aqueous Cd as the toxic metal. The first set of experiments was used to
139 test the responses and detoxification ability of *P. putida* cells to low concentrations of toxic Cd.
140 Bacteria were first cultured aerobically in 1 mL of Cd-free Lysogeny Broth (LB10) medium at 32
141 °C for 24 h, and were then transferred to 50 mL of LB10 medium containing 0, 5, or 20 ppm Cd,
142 and allowed to grow at the same temperature for 72 h. The LB10 medium consists of 10 g/L
143 tryptone, 5 g/L yeast extract and 10 g/L NaCl, and the Cd concentrations of the growth media were
144 attained by adding appropriate volumes of a 2 g/L Cd stock solution which was prepared by
145 dissolving Cd(NO₃)₂ in ultrapure water, and which was then sterilized by passing it through a 0.2
146 µm nylon filter membrane. Because of the high concentration of Cl⁻ in the medium, the Cd in the
147 LB10 medium is present primarily as relatively non-toxic aqueous Cd-chloride complexes
148 (Deheyn et al., 2004; Yu and Fein, 2015), and only a small percentage of the Cd is present in the
149 toxic form as free Cd²⁺ (Sunda et al., 1978). The optical density of the cell suspensions at 600 nm
150 (OD₆₀₀) was measured at different time intervals on a Cary 300 UV-Vis spectrophotometer and
151 the OD₆₀₀ value of the LB10 medium was used as a background value to calculate the increase in
152 OD₆₀₀ caused by the growth of *P. putida*. Abiotic control experiments using LB10 medium only
153 were also conducted under the same conditions in order to monitor if contamination occurs, and
154 the measured OD₆₀₀ values in these controls did not change within 72 h.

155 The second set of experiments was conducted to test the effects of cell surface sulfhydryl
156 sites on Cd toxicity towards *P. putida* cells. In order to yield biomass with different concentrations
157 of cell surface sulfhydryl sites, we used starter cells that were pre-cultured in Cd-free LB10
158 medium for 5, 6, 12, 24, or 72 h. The cell surface sulfhydryl site concentration for each biomass
159 sample was quantified using a potentiometric titration approach as described in Section 2.3. In
160 these toxicity experiments, we used a modified Lysogeny Broth medium (LB0.5) that consisted of
161 a similar formula to the LB10 medium except the NaCl content was reduced to 0.5 g/L in order to
162 decrease the prevalence of relatively non-toxic Cd-chloride aqueous complexes in the
163 experimental solutions and to increase the importance of Cd²⁺, which is toxic to the bacteria. The
164 experiments involved the addition of 0, 2, 5, 10, or 20 ppm Cd to the LB0.5 medium. While the
165 presence of tryptone and yeast extract makes the calculation of the Cd speciation in LB media
166 difficult, we calculated the speciation of Cd in 10 g/L and 0.5 g/L NaCl solutions using FITEQL
167 2.0 (Westall, 1982). At any Cd concentration used in this study (2, 5, 10 or 20 ppm), we found that
168 free Cd²⁺ accounts for 11% of the total aqueous Cd in 10 g/L NaCl and 64% of the total aqueous
169 Cd in 0.5 g/L NaCl. These calculations suggest that the reduction of the NaCl concentration from
170 10 g/L to 0.5 g/L significantly increases the concentration of free Cd²⁺ in the LB medium. In order
171 to compare the toxicity response of the cells with and without sulfhydryl sites blocked for Cd
172 binding, additional experiments (referred to below as '24h-Q' experiments) were conducted in the
173 presence of 20 ppm monobromo(trimethylammonio)-bimane bromide (qBBBr; from Toronto
174 Research Chemical) and 0 or 2 ppm Cd using starter cells that were pre-cultured for 24 h in LB10
175 medium. qBBBr selectively and irreversibly reacts with sulfhydryl sites on bacterial cell surfaces,
176 thus blocking them for Cd binding (Yu et al., 2014; Yu and Fein, 2015; Yu and Fein, 2017b).
177 Besides these changes, the conditions for the second set of experiments were the same as those

178 used in the first set of toxicity experiments previously described. Each of these toxicity
179 experiments was conducted in triplicate and the Student's t-test was applied to the results to test
180 for statistical significance.

181

182 **2.2 Extended X-ray absorption fine structure (EXAFS) measurements**

183 We used EXAFS measurements of the binding environment of Cd as a function of growth
184 stage in order to determine whether a relationship exists between the binding environment and the
185 measured toxicity response. Cells for the EXAFS experiments were grown in LB10 medium in the
186 presence of 20 ppm Cd, and were harvested at early exponential, early stationary and stationary
187 phases by centrifugation at $10,970 \times g$ for 5 min. In order to avoid Cd desorption from the biomass,
188 EXAFS measurements were conducted without cell washing. Cd K edge (26,711 eV) EXAFS was
189 measured in fluorescence mode using the third harmonic of the undulator at sector 10-ID beamline
190 of the Advanced Photon Source at Argonne National Laboratory (Segre et al., 2000). The energy
191 of the incident X-rays was scanned using a Si(111) reflection plane of a cryogenically-cooled
192 double-crystal monochromator. A Pt-coated mirror was used to remove X-rays of higher harmonic
193 energies. The incident ionization chamber was filled with 100% N₂ gas. The transmitted and
194 reference ion chambers were filled with 100% Ar gas. The fluorescence detector in the Stern–
195 Heald geometry (Stern and Heald, 1983) was filled with Kr gas, and a Pd filter of six absorption
196 lengths was used to reduce the background signal. Bacterial pellets were loaded into a slotted
197 Plexiglas holder, covered with Kapton film, and transported immediately to the beamline for
198 EXAFS measurements. All of the EXAFS measurements were performed within a day of the
199 sample preparation, and the samples were refrigerated prior to the EXAFS measurements. Quick

200 scans were used with signal sampling every 0.5 eV and with an integration time of 0.1 second per
201 point.

202 The X-ray absorption near edge structure (XANES) for each sample was monitored for
203 possible beam induced chemistry (and none was found), and the X-ray beam was moved to a fresh
204 spot every 5 scans in order to further reduce the possibility of radiation-induced changes and to
205 account for sample inhomogeneity. A total of 30–50 consecutive scans from each sample were
206 collected and averaged, with Cd foil data collected simultaneously in the reference chamber. Data
207 were analyzed using the UWXAFS package (Stern et al., 1995). Processing of the raw data,
208 including alignment of datasets and background removal, was done using ATHENA (Ravel and
209 Newville, 2005). The input parameter to ATHENA that determines the maximum frequency of the
210 background, R_{bkg} , was set to 1.1 Å (Newville et al., 1993). The data range used for Fourier
211 transforming the EXAFS data was 3.0–9.8 Å⁻¹ with a Hanning window function and a dk value of
212 1.0 Å⁻¹ (Newville et al., 1993). Simultaneous fitting of each of the three datasets with multiple k-
213 weighting (k^1 , k^2 , k^3) of each spectrum was performed using the Fourier transformed spectra. The
214 fitting range for all of the datasets was 1.2–2.8 Å. The simultaneous fitting approach reduces the
215 possibility of obtaining erroneous parameters due to correlations at any single k-weighting (Mishra
216 et al., 2010).

217 The EXAFS spectra from Cd-acetate, Cd-phosphate, and Cd-sulfide standards were used
218 for qualitative comparison of the unknown samples, and these same spectra were also used to
219 refine fitting parameters for the quantitative analysis of the Cd binding environment in the biomass
220 samples. The best fit values for the O and S signal contributions to the EXAFS spectra from the
221 standards were used as the initial guess parameters for simultaneous fitting of the three biomass
222 samples. The relative contributions of Cd-S and Cd-O binding to the total Cd binding environment

223 within the first shell of the biomass samples were determined by floating the O coordination
224 number and constraining the S coordination number such that the total contribution of the two sites
225 would sum to be 100%. Because O coordinates octahedrally around a Cd atom, and S coordinates
226 tetrahedrally, it was assumed that full coordination of the O-bearing and S-bearing sites was 6 O
227 and 4 S atoms, respectively. In this analysis, we do not differentiate between carboxyl and
228 phosphoryl binding sites because the Cd-O bond distances in the Cd-acetate and Cd-phosphate
229 standards are the same (Mishra et al., 2010). An attempt to performed EXAFS fits using
230 contribution from Cd-phosphate, Cd-acetate, and Cd-sulfide signals resulted in statistically inferior
231 fits suggesting that inclusion of Cd-phosphate in addition to Cd-acetate and Cd-sulfide is not
232 justified for a statistically meaningful fitting of biomass data. Therefore, we did not include the
233 Cd-phosphate standard in our modeling.

234 **2.3 Determination of sulfhydryl sites on bacterial cell surfaces**

235 The preparation of the biomass samples that were used for sulfhydryl site measurements
236 was as follows: after incubation in Cd-free LB10 medium at 32 °C for different periods of time (5,
237 6, 12, 24, or 72 h), the biomass was harvested by centrifugation at 10,970 $\times g$ for 5 min. The
238 biomass pellets were then washed three times with a 0.1 M NaCl solution, with centrifugation at
239 8,100 $\times g$ for 5 min after each wash. The biomass pellets were then transferred into pre-weighed
240 test tubes and centrifuged for two 30-minute intervals at 8,100 $\times g$. After decanting the supernatant,
241 the wet weight of the biomass was used to calculate the bacterial concentrations in the subsequent
242 experiments, and the bacterial concentrations that are reported in this study are these wet weights.

243 Some experiments involved bacterial cells with EPS materials removed. In order to remove
244 EPS from biomass samples, the freshly harvested and washed cell pellets were immediately re-
245 suspended in 0.1 M NaCl with a cation exchange resin (Dowex® Marathon C sodium form, 20-

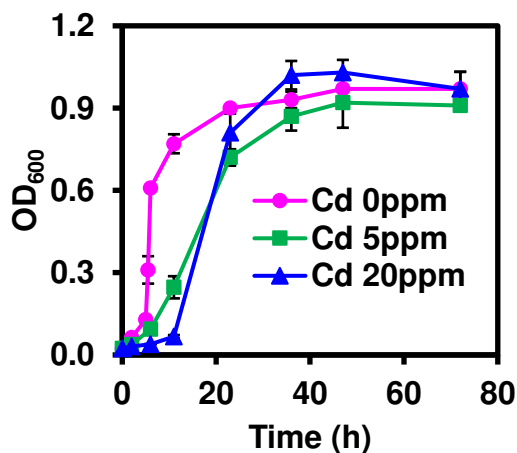
246 50 mesh, 30 g of resin/g of biomass in wet weight) and allowed to react for 2 h at room temperature
247 (~20 °C) with slow stirring in order to maintain homogeneous suspensions. The treated cells were
248 then washed using the same procedure as described above. The biomass that is produced from this
249 resin treatment procedure is virtually free of EPS materials, as previous studies have demonstrated
250 with electron microscopy (Yu and Fein, 2016).

251 The approach used to determine the sulfhydryl site concentrations on bacterial cell surfaces was
252 the same procedure that we developed and described in previous studies (Yu et al., 2014; Yu and
253 Fein, 2017a). We used potentiometric titrations and surface complexation modeling to determine
254 the total site concentrations within biomass samples. The concentration of sulfhydryl sites was
255 determined by measuring the decrease in the total concentration of all binding sites after the
256 sulfhydryl sites were selectively blocked using monobromo(trimethylammonio)-bimane bromide
257 (qBBr), a molecule that itself does not protonate or deprotonate. In order to block sulfhydryl sites,
258 cells were suspended for 2 h in a freshly prepared qBBr solution in 0.1 M NaCl with pH buffered
259 to 7.0 ± 0.1 using a 1.8 mM Na_2HPO_4 /18.2 mM NaH_2PO_4 buffer, with a qBBr:biomass ratio of
260 approximately 200 $\mu\text{mol/g}$, followed by three biomass washes with a 0.1 M NaCl electrolyte
261 solution. Potentiometric titrations of cells with and without qBBr treatment were conducted using
262 an autotitrator assembly with ~10 g of a 0.1 M NaCl cell suspension containing 30 g (wet mass)
263 of cell per liter. The cell suspensions were first adjusted to pH 3.0 using 1 M HCl, followed by a
264 titration from pH 3.0 to 9.7 using 1M NaOH. The ‘up pH’ titration was used for calculating the
265 total bindings sites on each sample using a four-site non-electrostatic surface complexation model
266 and FITEQL 2.0. All titrations were conducted in triplicate.

267

268 **3. Results**

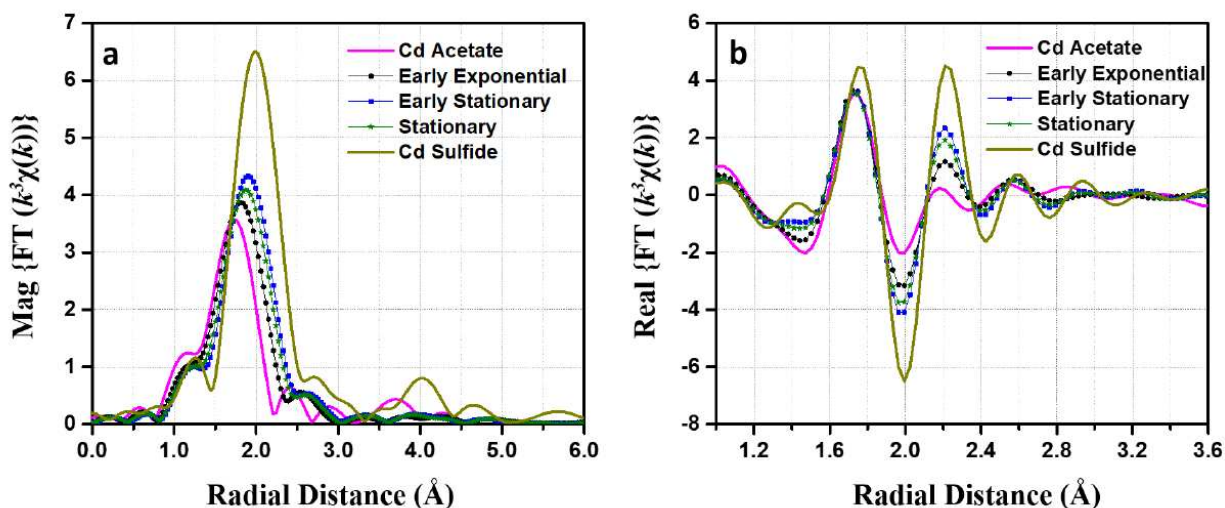
269 The presence of 5 or 20 ppm Cd in LB10 medium caused strong negative effects on the
270 growth of *P. putida* within the first few hours of the experiment, but did not affect the extent of
271 overall growth in the long term (Figure 1). When the Cd concentration in the growth medium
272 increased from 0 to 20 ppm, the lag phase of *P. putida* extended markedly from about 5 h to 12 h.
273 However, in each case, once the lag phase was complete, cells in each of the three experiments
274 multiplied rapidly. After 24 hours, similar OD₆₀₀ values were observed for cell suspensions in the
275 presence of 0, 5 and 20 ppm Cd, indicating that *P. putida* cells completely detoxified the added Cd
276 in these experiments. In LB10 medium, most of the Cd is present as aqueous Cd-chloride
277 complexes (e.g., CdCl⁺, CdCl₂⁰), and only <11% of the Cd is present as relatively toxic Cd²⁺.
278 Therefore, our results show that *P. putida* cells are sensitive to very low concentrations of toxic
279 Cd species, and that the cells can detoxify at least low concentrations of Cd²⁺.
280



281
282 **Figure 1.** Growth curves of *P. putida* in LB10 media containing 0, 5, or 20 ppm Cd.
283
284
285 The EXAFS analysis of the *P. putida* biomass samples that grew in the presence of 20 ppm
286 Cd in LB10 medium indicates that a significant amount of Cd adsorbed onto the biomass, and that
287 the adsorbed Cd was partitioned between complexation with sulfur- and oxygen-bearing binding

288 sites (Figure 2). The Cd-sulfide spectrum exhibits a first shell (Cd-S) peak that is shifted to a
 289 significantly larger distance and amplitude relative to those associated with the first shell (Cd-O)
 290 peak from the spectrum for the Cd-acetate standard (Figure 2a). In addition, the amplitude of the
 291 peak at 2.2 Å is larger in the real part of the Cd-sulfide EXAFS spectrum than it is in the Cd-
 292 acetate spectrum (Figure 2b). These spectral features can be used to qualitatively determine the
 293 relative contributions of Cd-O and Cd-S bonds to the total adsorbed Cd on the biomass (Mishra et
 294 al., 2010).

295



296

297 **Figure 2.** (a) Magnitude and (b) real part of the Fourier transform of the measured Cd K-edge
 298 EXAFS spectra of three biomass samples compared to Cd-acetate and Cd-sulfide standards. The
 299 biomass samples were grown in LB10 medium in the presence of 20 ppm Cd and harvested at
 300 early exponential, early stationary and stationary phase.

301

302

303 The EXAFS spectra of the three biomass samples indicate a significant increase in the
 304 importance of Cd-S binding as the growth phase progresses from early exponential to early
 305 stationary phase, followed by a small decrease in the importance of Cd-S binding from early
 306 stationary to stationary phase (Figure 2). Quantitative modeling of the Cd EXAFS data with both

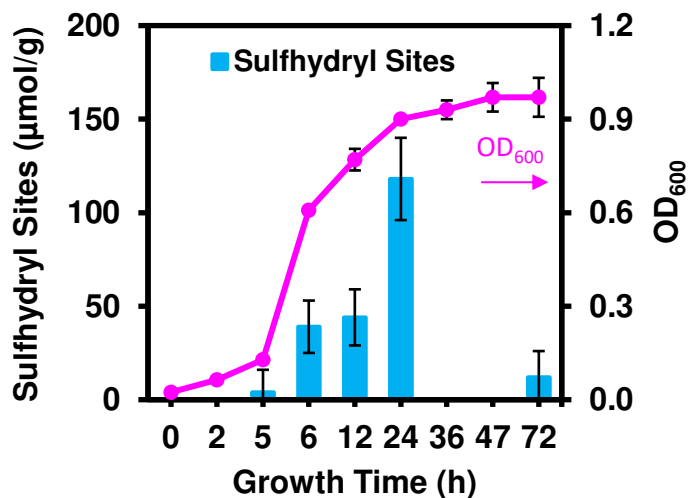
307 Cd-O and Cd-S paths yields excellent fits to the data (Figure S1 and S2, Table 1 and S1). For the
 308 early exponential phase sample, O-bearing (non-sulfhydryl) binding sites dominate Cd adsorption
 309 onto the biomass, and only 18% of the adsorbed Cd on the biomass is bound to S-bearing
 310 (sulfhydryl) binding sites (Table 1). In contrast, the calculated contribution of the S-bearing
 311 binding sites increases markedly to 51% in the early stationary phase sample (Figure S2 and Table
 312 1), and then decreases slightly with extended growth time to 40% in the stationary phase sample.

313
 314 **Table 1.** Relative contribution of Cd binding from O- and S-bearing sites on *P. putida* biomass
 315 samples that grew in the presence of 20 ppm Cd.
 316

Growth Phase	Cd-O (%)	Cd-S (%)
Early Exponential	82 ± 5	18 ± 5
Early Stationary	49 ± 9	51 ± 8
Stationary	60 ± 7	40 ± 7

317
 318 We used potentiometric titration experiments to measure the concentrations of sulfhydryl
 319 sites on cell surfaces of *P. putida* biomass that were cultured in Cd-free LB10 media, and were
 320 sampled at different points along its growth curve. The abundance of sulfhydryl sites is strongly
 321 affected by growth phase (Figure 3 and Table S2). From early exponential phase (5 h) to early
 322 stationary phase (24 h), the measured concentration of sulfhydryl sites on the cell surfaces
 323 increases dramatically from 4±12 to 118±22 μmol/g, likely explaining the increase in Cd-
 324 sulfhydryl binding on biomass samples from exponential phase to stationary phase that was
 325 documented by our EXAFS measurements (Figure 2 and Table 1). In contrast, the measured
 326 sulfhydryl site concentration for late stationary phase (72 h) cells is only 12±14 μmol/g. However,
 327 it should be noted that the measured total concentrations of sulfhydryl sites from the potentiometric
 328 titration experiments are for samples grown in Cd-free media, and that the presence of Cd could

329 potentially induce the synthesis of additional sulfhydryl sites by bacterial cells. Therefore a direct
330 linkage of the measured sulfhydryl site concentrations to the relative importance of Cd-sulfhydryl
331 binding at each growth phase as determined by EXAFS is not possible.
332



333
334 **Figure 3.** Potentiometric titration measurement results of the concentrations of cell surface
335 sulfhydryl sites on *P. putida* biomass at different growth stages that were cultured in Cd-free LB10
336 medium. Note the non-linear scale to the ‘Growth Time’ axis.

337
338
339
340 The above measurements were all conducted with intact biomass samples, which included
341 both cells and bound EPS material. In order to identify the location of the sulfhydryl sites between
342 the cell walls and cell-produced EPS material for the 24h-biomass, we removed the EPS material
343 through a cation exchange resin pre-treatment (Yu and Fein, 2016), and measured the surface
344 sulfhydryl sites on the biomass without EPS. After the EPS was removed, the measured
345 concentrations of sulfhydryl sites on the cell surfaces dropped dramatically from 118 ± 22 to 4 ± 18
346 $\mu\text{mol/g}$ (Table S2). This result, similar to the findings in previous potentiometric titration and
347 proteomic analyses for *P. putida* (Yu and Fein, 2016; Fein et al., 2019), indicate that the sulfhydryl
348 sites on cell surfaces of *P. putida* under our growth conditions are located mainly on the EPS

349 molecules that are tightly bound to cells. Bacterial cells synthesize EPS primarily from mid-
350 exponential phase to early stationary phase (Petry et al., 2000; Lbarburu et al., 2007). Therefore,
351 the extremely low concentrations of sulfhydryl sites on the surfaces of the early exponential phase
352 (5 h) cells likely arise because the cells did not yet synthesize EPS molecules at this growth stage.
353 Although abundant sulfhydryl sites were detected on the 24 h biomass, the concentration of
354 sulfhydryl sites on the 72 h biomass decreased dramatically (Figure 3). We interpret these results
355 to indicate that sulfhydryl-bearing EPS molecules likely detach from the cell surfaces upon the
356 death and degradation of the 24h-cells, and that newly synthesized cells which contain much lower
357 concentrations of bound sulfhydryl-rich EPS molecules become the dominant cells at late
358 stationary phase (72 h), resulting in the low sulfhydryl site concentration of the 72h-cells sample.

359 The second set of toxicity experiments used an LB0.5 medium containing only 0.5 g/L
360 NaCl, and starter biomass that was extracted from growth in an LB10 medium at different stages
361 along the growth curve. Hence, each starter biomass contained different concentrations of cell
362 surface sulfhydryl sites (Figure 3). Because starter cells with different pre-culturing times exhibit
363 different lag phases and growth rates when placed in the Cd-free LB0.5 medium, in order to
364 compare the effects of Cd toxicity on each type of biomass, we report cell growth in terms of
365 growth factor values that are calculated as the OD₆₀₀ of a cell suspension in the presence of Cd
366 divided by the OD₆₀₀ in corresponding Cd-free controls. A growth factor of 1 indicates that the
367 added Cd has no effect on the growth of bacterial cells, and lower growth factor values indicate
368 stronger Cd toxicity.

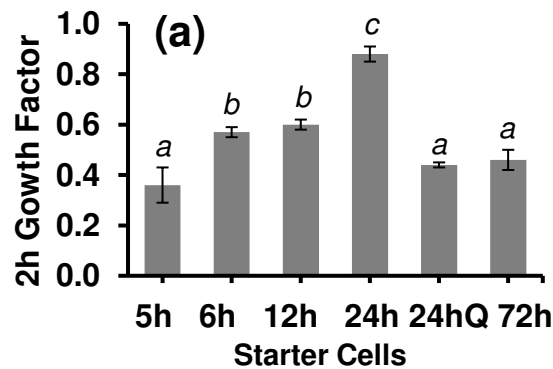
369 In contrast to the minor influence of 20 ppm Cd on the growth of *P. putida* in the LB10
370 medium (Figure 1), the presence of 2-20 ppm Cd strongly inhibits the growth of *P. putida* in the
371 LB0.5 medium due to the dramatically increased concentration of free Cd²⁺, with growth factors

372 in most experiments smaller than 0.6 (Figure S3). The pre-culturing time of the starter cells exerts
373 a strong influence on the toxicity of Cd toward the cells, and the influence decreases with duration
374 of the toxicity experiment. For example, at 2 h in the toxicity experiments in the presence of 2 ppm
375 Cd, the growth factors in the different experiments vary markedly from 0.3 to 0.9, but these
376 differences become negligible at 24 h (Figure S3). Similar trends are also observed in experiments
377 in the presence of elevated Cd concentrations (Figure S3). The decreasing difference in growth
378 factors for the different starter cells with increasing time likely occurs because the proportion of
379 newly produced *P. putida* cells keeps increasing with time in each experiment, and the properties
380 of these newly created cells are independent of the pre-culturing time of the starter cells. That is,
381 as the toxicity experiment proceeds, the starter cells become a smaller proportion of the total
382 number of cells in each experiment, and hence the differences in growth disappear with increasing
383 time. Therefore, because the objective of this set of experiments is to study the influence of the
384 surface sulfhydryl site concentration on Cd toxicity to *P. putida*, we focus on the growth factors
385 of the *P. putida* cells at 2 h because at that time the experimental systems have the largest
386 proportion of starter cells present and hence best represent the toxic response of the starter cells
387 (with different sulfhydryl site concentrations) to Cd.

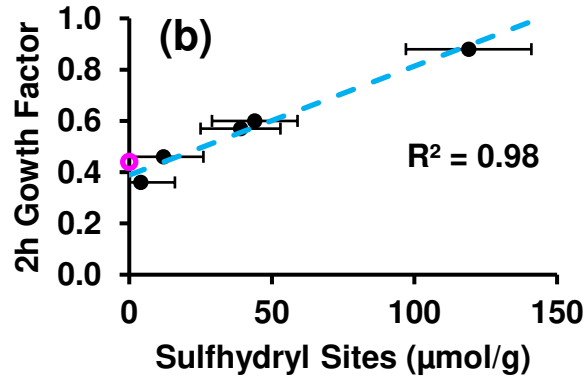
388 Among the different batches of starter cells, the 24h-cells (the cells that were pre-cultured
389 for 24 h in LB10 medium), which have the highest concentration of cell surface sulfhydryl sites
390 (Figure S3), always showed the lowest toxicity responses to Cd, with 2h growth factors
391 significantly higher than other experiments at any studied Cd concentration (Figure S3). In contrast,
392 the 5h-cells that contain the lowest concentration of sulfhydryl sites exhibited the smallest 2 h
393 growth factors (Figure S3), with their growth completely inhibited at 2 h in the presence of 5, 10
394 or 20 ppm Cd (2h growth factors = 0). Based on the Student's t-test results for the 2h growth

395 factors of different starter cells, the starter cells can be divided into three groups, with 2h growth
396 factors for the 5h- and 72h-cells lower than the growth factors for the 6h- and 12h-cells, which in
397 turn are lower than the growth factors of the 24h-cells (Figure 4a). Here the 2h growth factors of
398 any two starter cells from different groups are significantly different ($p < 0.05$), and those from the
399 same group show no statistical difference ($p > 0.05$). For the 24h-cells, we also conducted a
400 comparison experiment in the presence of qBBr, a molecule that selectively and irreversibly blocks
401 cell surface and EPS sulfhydryl sites to interactions with Cd in the experiment. In this experiment
402 (24hQ), with sulfhydryl binding sites blocked, the toxicity of 2 ppm Cd to the cells was
403 significantly higher than was observed in the qBBr-free experiments, with the 2h growth factor
404 dropping from 0.88 ± 0.03 for the qBBr-free experiment to 0.44 ± 0.01 for the qBBr experiment
405 ($p < 0.05$, Figure 4a).

406
407
408
409
410
411
412
413
414
415
416

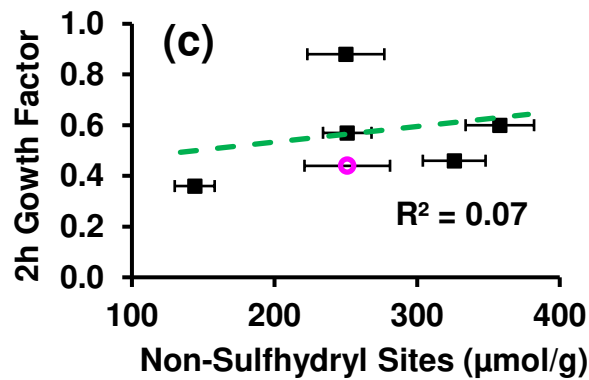


417
418



419

420



421

422

423 **Figure 4.** Toxicity test results in LB0.5 medium that contains 2 ppm Cd using *P. putida* starter
 424 cells that were pre-cultured in LB10 medium for 5 h, 6 h, 12 h, 24 h or 72 h, reported in terms of
 425 the 2h growth factor, which is calculated by normalizing the OD₆₀₀ of a cell suspension at 2 h in a
 426 Cd-bearing experiment by the OD₆₀₀ in the Cd-free control at 2 h. The 24h-Q experiment was
 427 conducted using the 24h-cells as starter cells in the presence of qBBr that blocks cell surface
 428 sulfhydryl sites to Cd binding. (a) The 2h growth factor values using starter cells from different
 429 extraction times from the parent growth medium; (b) Relationship between measured 2h growth
 430 factor values and measured cell surface sulfhydryl site concentrations on the starter biomass; (c)
 431 Relationship between measured 2h growth factor values and measured concentrations of the non-
 432 sulfhydryl sites on the starter biomass. The letters on top of each column in (a) represent the
 433 Student's t-test results: $p < 0.05$ for any two samples with different letters and $p > 0.05$ for any two
 434 samples with the same letters. The pink hollow circles in (b) and (c) represent the results of the
 435 24hQ experiment.

436

437

438

439 By plotting the sulfhydryl site concentrations of the starter cells with their 2h growth
 factors in the presence of 2 ppm Cd, we find a strong positive correlation between the growth

440 factors and the sulfhydryl site concentrations of the starter cells (Figure 4b, $R^2=0.98$). It is
441 noteworthy that the growth factor in the 24hQ qBBr experiment with the sulfhydryl sites on the
442 24h-cells blocked matches well with the predicted growth factor for starter cells with no cell
443 surface sulfhydryl sites (pink circle in Figure 4b). In contrast, the 2h growth factors exhibit a poor
444 correlation to the concentrations of the non-sulfhydryl sites on the biomass samples, which include
445 all of the other binding sites on the cell surfaces (Figure 4c, $R^2=0.07$). The observed correlation is
446 not limited to the 2 ppm Cd dataset, as the measured 2h growth factors in the 5, 10, and 20 ppm
447 Cd experiments all exhibit strong correlations with cell surface sulfhydryl site concentrations
448 (Figure S4). The goodness of the correlations decreases in general with increasing Cd
449 concentrations, likely because for the experiments with higher total Cd concentrations, the
450 concentration of adsorbed Cd exceeds the concentration of sulfhydryl binding sites, and Cd in
451 these systems also binds to some extent to non-sulfhydryl sites under these elevated metal loadings
452 (Mishra et al., 2010; Yu and Fein, 2015; Nell and Fein, 2017). This result is consistent with
453 sulfhydryl sites playing a crucial role in diminishing Cd toxicity, and for the high Cd systems in
454 which significant non-sulfhydryl binding occurs, Cd toxicity increases and the relationship
455 between sulfhydryl site concentration and Cd toxicity breaks down to some extent.

456 **4. Discussion**

457 An important finding of this study is that the *P. putida* cells cultured in the LB10 medium
458 contain relatively high concentrations of sulfhydryl sites on their cell surfaces compared to
459 sulfhydryl site concentrations that have been measured for other bacterial species (Joe-Wong et
460 al., 2012; Yu et al., 2014; Yu and Fein, 2016; Yu and Fein, 2017a). For example, the measured
461 concentration of surface sulfhydryl sites on the *P. putida* cells that were cultured in LB10 medium
462 to early stationary phase (the 24h sample in Figure 3) is $118 \pm 22 \mu\text{mol/g}$, which is at least three-

463 fold higher than the reported values for most other bacterial species that have been studied (Joe-
464 Wong et al., 2012; Yu et al., 2014; Yu and Fein, 2016; Yu and Fein, 2017a), including *P. putida*
465 cells that were grown in a nutrient-rich TSB medium (Yu et al., 2014; Yu and Fein, 2017a) and a
466 M9 minimal medium (Yu and Fein, 2017a). Although it is not clear why the *P. putida* cells contain
467 such high concentrations of cell surface sulfhydryl sites when they are cultured in the LB10
468 medium, Choi et al. (2014) found that *P. putida* cells cultured in the LB10 medium have more than
469 a three-fold higher protein content within their EPS matrix compared to *P. putida* cells grown in
470 two other minimal media. Proteins are likely the primary hosts of sulfhydryl sites both within cell
471 envelopes and on EPS material (Norrod et al., 1993; Fein et al., 2019). Therefore, our findings
472 suggest that the energy source and perhaps other environmental factors during cell growth play
473 important roles in the production of surface proteins and hence cell surface sulfhydryl binding sites
474 by *P. putida* (Choi et al., 2014). Further studies aimed at identifying the factors that control
475 sulfhydryl-bearing protein production and distribution, and their influence on heavy metal toxicity
476 to other bacterial species are crucial.

477 The high concentration of sulfhydryl sites on the cell surface of *P. putida* leads to Cd-
478 sulfhydryl binding representing a large proportion of the total adsorbed Cd budget under high Cd
479 loading conditions (Table 1). Typically, because of the limited abundance of high affinity
480 sulfhydryl binding sites on bacteria, metal-sulfhydryl binding decreases in importance when metal
481 loadings exceed approximately 10 $\mu\text{mol/g}$ (Guine et al., 2006; Mishra et al., 2010; Pokrovsky et
482 al., 2012; Yu and Fein, 2015; Nell and Fein, 2017). However, our EXAFS analysis indicates that
483 Cd-sulfhydryl binding represents over 50% of the total adsorbed Cd budget in the early stationary
484 phase biomass sample (Figure S2, Table 1) which was exposed to a metal loading of approximately
485 130 $\mu\text{mol/g}$. Most bacterial species that have been studied exhibit cell surface sulfhydryl site

486 concentrations of 20 – 40 $\mu\text{mol/g}$ (Joe-Wong et al., 2012; Yu et al., 2014; Mishra et al., 2017; Yu
487 and Fein, 2017a). In two cases, much higher concentrations have been reported: $93 \pm 8 \mu\text{mol/g}$ for
488 *Bacillus subtilis* cells that were grown in a TSB medium containing 50 g/L of glucose (Yu and
489 Fein, 2017a), and $68 \pm 23 \mu\text{mol/g}$ for *Geobacter sulfurreducens* cells that were grown in a fresh
490 basal medium (Mishra et al., 2017). Similar to the finding of this study, sulfhydryl sites were shown
491 to play an important role in the adsorption of metals onto these biomass samples even under
492 relatively high metal loadings, ranging from 20-50 $\mu\text{mol/g}$ (Mishra et al., 2017; Yu and Fein,
493 2017b).

494 In addition to the high abundance of sulfhydryl sites, the location of the sulfhydryl sites
495 primarily on EPS molecules also contributes to the dominance of Cd-sulfhydryl complexes on cell
496 surfaces of the *P. putida* cells. Aqueous metals interact with biomass first through interactions
497 with EPS molecules due to their location on the outermost layers of the cell surface. If EPS
498 molecules contain a higher ratio of sulfhydryl sites relative to other possible metal binding sites
499 than does the bacterial cell envelope, then Cd-sulfhydryl binding will be favored even under higher
500 metal loadings than would be the case if the sulfhydryl sites were located within the cell envelope
501 with the plentiful other non-sulfhydryl binding sites.

502 The sulfhydryl sites on *P. putida* EPS molecules dominate Cd adsorption onto bacterial
503 biomass under the experimental conditions. In so doing, we conclude that the sites also play an
504 important role in detoxification of Cd by sequestering the metal on EPS molecules and away from
505 the cell walls where internalization could occur. Cd^{2+} ions can readily bind to dissolved thiols, and
506 the conversion in solution of free Cd^{2+} or weak Cd complexes to Cd-thiol complexes can
507 dramatically reduce the toxicity of Cd to bacteria (Murata et al., 1985). Similarly, the binding of
508 Cd to the sulfhydryl sites on cell-bound EPS of *P. putida* can also reduce the toxicity of Cd.

509 Because of the strength of the Cd-S bond, the adsorbed Cd is likely relatively inert within the EPS
510 matrix, and remains so until the EPS molecule that hosts the sulfhydryl site is degraded. In fact,
511 previous studies (Rubino, 2015) find that CdS is the only Cd product for the degradation of Cd-
512 metallothionein complexes and no free Cd²⁺ is released during the whole degradation, indicating
513 that the adsorbed Cd onto the sulfhydryl sites of EPS likely remains nontoxic after the degradation
514 of EPS molecules at least in some cases. In contrast, the complexes between Cd²⁺ and other binding
515 sites (e.g., carboxyl and phosphoryl sites) are significantly weaker (Yu and Fein, 2015), and hence
516 the adsorbed Cd²⁺ that is bound to these non-sulfhydryl sites can easily desorb and thus remains
517 potentially toxic to the bacterial cells. As a result, we observed no correlation between the extent
518 of Cd toxicity and the concentrations of non-sulfhydryl sites on *P. putida* cell surfaces (Figure 4C
519 and Figure S4).

520 *P. putida* cells possess multiple types of detoxification systems, enabling them to survive
521 a range of extreme or contaminated environments (Murata et al., 1985; Chen et al., 1995; Shamim
522 et al., 2014). This study elucidates one of these methods of detoxification. *P. putida* cells produce
523 EPS molecules that are bound to the bacterial cells and which contain high concentrations of
524 sulfhydryl binding sites. When *P. putida* biomass is exposed to aqueous Cd, our experiments
525 demonstrate that the Cd becomes bound to these EPS-hosted sulfhydryl sites (Figure 2), decreasing
526 the toxicity of the Cd to the *P. putida* cells. Biomass from different growth stages contains different
527 amounts of EPS (Petry et al., 2000; Lbarburu et al., 2007), and hence different concentrations of
528 sulfhydryl sites (Figure 3). Our experiments demonstrate that the extent of Cd toxicity to the
529 bacterial cells is inversely related to the concentration of sulfhydryl sites on bacterial cell surfaces
530 (Figure 4b). In addition to Cd, the sulfhydryl sites on the cell surfaces of *P. putida* likely can reduce
531 the toxicity of a range of other chalcophile or similar metals as well, such as Hg, Zn, Au and Cu,

532 because these metals also strongly bind to sulfhydryl sites (Guine et al., 2006; Pokrovsky et al.,
533 2012; Nell and Fein, 2017; Yu and Fein, 2017b). It is unclear at this time how widespread this
534 detoxification strategy is among bacterial species, but sulfhydryl sites have been detected on the
535 EPS molecules within the biofilms that are produced by some pathogenic bacteria (*Pseudomonas*
536 *aeruginosa*, *Staphylococcus aureus* and *Escherichia coli*) and biofilm formation bacteria on
537 drinking water pipes (*Pleomorphomonas oryza NMI* and *Acidovorax ebreus NM25*) (Lin et al.,
538 2014), with the roles of their EPS sulfhydryl sites unexplored. Therefore, further studies focusing
539 on the potential role of cell surface sulfhydryl sites of these bacterial species in detoxification
540 would be important for addressing multiple key environmental issues, such as water disinfection
541 and drinking water pipe protection. Some species, such as *Shewanella oneidensis*, produce EPS
542 molecules with much lower concentrations of sulfhydryl sites than does *P. putida*, and cell
543 envelopes with much higher concentrations (Yu and Fein, 2016), and hence likely rely on other
544 strategies than EPS metal sequestration for metal detoxification. However, it is noteworthy that
545 the sulfhydryl sites on EPS molecules of *P. putida* could also contribute to protect other microbial
546 species from toxic metals in natural environments, where mixed microbial species form aggregates
547 such as biofilms and microbial mats via the production of EPS.

548 The decrease in sulfhydryl site concentration in the biomass samples from 24 h to 72 h
549 (Figure 3) suggests that, under the experimental conditions studied, EPS molecules can mobilize
550 from planktonic bacterial cells upon death and degradation of the cells. However, EPS molecules
551 within biofilms are likely to be more stable and remain immobile until the whole biofilm collapses,
552 especially those EPS molecules located in the biofilm interior. The degree of mobilization may
553 greatly affect the stability and lifespan of EPS-associated sulfhydryl binding sites. For example,
554 previous studies found that although sulfhydryl sites on small molecules such as cysteine oxidize

555 rapidly when exposed to air (Hird and Yates, 1961), but significantly less oxidation occurs when
556 the cysteine is present in the outer layers of a biofilm, and no oxidation of cysteine occurs in the
557 inner layers of biofilms (Lin et al., 2014). Therefore, sulfhydryl sites within the bacterial biofilms
558 that are ubiquitous in natural environments likely play a more important and long-lasting role in
559 metal detoxification than what we observed in our experiments for planktonic cells. In order to
560 determine the prevalence of EPS metal sequestration as a strategy for metal detoxification in
561 natural and engineered systems, it is crucial to expand study from isolated bacterial species to
562 natural bacterial consortia and biofilms to measure sulfhydryl site concentrations on cells relative
563 to that on EPS molecules, and to determine if a relationship exists, as we have observed for *P.*
564 *putida*, between sulfhydryl site concentrations and metal toxicity response.

565

566

567

568 **Acknowledgements**

569 QY was supported through the Center for Environmental Science and Technology at University
570 of Notre Dame. The research was funded in part by U.S. National Science Foundation grants EAR-
571 1424950 and EAR-1904192. Two journal reviews were helpful and significantly improved the
572 presentation of this work.

573

574

575 **Supporting Information Available**

576

577 **References**

578 Beveridge, T.J., Murray, R.G.E., 1976. Uptake and retention of metals by cell walls of *bacillus*
579 *subtilis*. J Bacteriol 127, 1502-1518.

580 Chandrangu, P., Rensing, C., Helmann, J.D., 2017. Metal homeostasis and resistance in bacteria.
581 Nat Rev Microbiol 15, 338-350.

582 Chen, J.H., Lion, L.W., Ghiorse, W.C., Shuler, M.L., 1995. Mobilization of adsorbed cadmium
583 and lead in aquifer material by bacterial extracellular polymers. Water Res 29, 421-430.

584 Chen, X., Shi, J., Chen, Y., Xu, X., Xu, S., Wang, Y., 2006. Tolerance and biosorption of copper
585 and zinc by *pseudomonas putida* cz1 isolated from metal-polluted soil. Canadian Journal of
586 Microbiology 52, 308-316.

587 Choi, C.W., Park, E.C., Yun, S.H., Lee, S.Y., Lee, Y.G., Hong, Y., Park, K.R., Kim, S.H., Kim,
588 G.H., Kim, S.I., 2014. Proteomic characterization of the outer membrane vesicle of *pseudomonas*
589 *putida* kt2440. J Proteome Res 13, 4298-4309.

590 Deheyn, D.D., Bencheikh-Latmani, R., Latz, M.I., 2004. Chemical speciation and toxicity of
591 metals assessed by three bioluminescence-based assays using marine organisms. Environ Toxicol
592 19, 161-178.

593 Fein, J.B., Yu, Q., Nam, J., Yee, N., 2019. Bacterial cell envelope and extracellular sulfhydryl
594 bindings: Their roles in metal binding and bioavailability. Chem Geol 521, 28-38.

595 Flynn, S.L., Szymanowski, J.E.S., Fein, J.B., 2014. Modeling bacterial metal toxicity using a
596 surface complexation approach. Chem Geol 374, 110-116.

597 Gadd, G.M., Griffiths, A.J., 1978. Microorganisms and heavy-metal toxicity. Microbial Ecol 4,
598 303-317.

599 Guine, V., Spadini, L., Sarret, G., Muris, M., Delolme, C., Gaudet, J.P., Martins, J.M.F., 2006.
600 Zinc sorption to three gram-negative bacteria: Combined titration, modeling, and exafs study.
601 Environmental Science & Technology 40, 1806-1813.

602 Higham, D.P., Sadler, P.J., Scawen, M.D., 1986. Cadmium-binding proteins in *pseudomonas-*
603 *putida* - pseudothioneins. Environ Health Persp 65, 5-11.

604 Hird, F.J.R., Yates, J.R., 1961. The oxidation of cysteine, glutathione and thioglycollate by iodate,
605 bromate, persulphate and air. Journal of the Science of Food and Agriculture 12, 89-95.

606 Hu, N., Zhao, B., 2007. Key genes involved in heavy-metal resistance in *pseudomonas putida* cd2.
607 FEMS Microbiology Letters 267, 17-22.

608 Joe-Wong, C., Shoenfelt, E., Hauser, E.J., Crompton, N., Myneni, S.C.B., 2012. Estimation of
609 reactive thiol concentrations in dissolved organic matter and bacterial cell membranes in aquatic
610 systems. Environmental Science & Technology 46, 9854-9861.

611 Lbarburu, I., Soria-Diaz, M.E., Rodriguez-Carvajal, M.A., Velasco, S.E., Tejero-Mateo, P., Gil-
612 Serrano, A.M., Irastorza, A., Duenas, M.T., 2007. Growth and exopolysaccharide (eps) production
613 by *oenococcus oeni* i4 and structural characterization of their eps. J Appl Microbiol 103, 477-486.

614 Li, Q.L., Mahendra, S., Lyon, D.Y., Brunet, L., Liga, M.V., Li, D., Alvarez, P.J.J., 2008.
615 Antimicrobial nanomaterials for water disinfection and microbial control: Potential applications
616 and implications. Water Res 42, 4591-4602.

617 Lin, H.R., Ye, C.S., Lv, L., Zheng, C.R., Zhang, S.H., Zheng, L., Zhao, Y.D., Yu, X., 2014.
618 Characterization of extracellular polymeric substances in the biofilms of typical bacteria by the
619 sulfur k-edge xanes spectroscopy. J Environ Sci-China 26, 1763-1768.

620 Liu, H., Fang, H.H.P., 2002. Characterization of electrostatic binding sites of extracellular
621 polymers by linear programming analysis of titration data. Biotechnol Bioeng 80, 806-811.

622 Liu, H.J., Wang, Y.Q., Zhang, H., Huang, G.D., Yang, Q.X., Wang, Y.L., 2019. Synchronous
623 detoxification and reduction treatment of tannery sludge using cr (vi) resistant bacterial strains.
624 Science of the Total Environment 687, 34-40.

625 Mishra, B., Boyanov, M., Bunker, B.A., Kelly, S.D., Kemner, K.M., Fein, J.B., 2010. High- and
626 low-affinity binding sites for cd on the bacterial cell walls of *bacillus subtilis* and *shewanella*
627 *oneidensis*. Geochim Cosmochim Ac 74, 4219-4233.

628 Mishra, B., Shoenfelt, E., Yu, Q., Yee, N., Fein, J.B., Myneni, S.C.B., 2017. Stoichiometry of
629 mercury-thiol complexes on bacterial cell envelopes. Chem Geol 464, 137-146.

630 Murata, K., Fukuda, Y., Shimosaka, M., Watanabe, K., Saikusa, T., Kimura, A., 1985. Phenotypic
631 character of the methylglyoxal resistance gene in *saccharomyces cerevisiae* - expression in
632 *escherichia coli* and application to breeding wild-type yeast strains. Appl Environ Microb 50,
633 1200-1207.

634 Nell, R.M., Fein, J.B., 2017. Influence of sulfhydryl sites on metal binding by bacteria. Geochim
635 Cosmochim Acta 199, 210-221.

636 Newville, M., Livins, P., Yacoby, Y., Rehr, J.J., Stern, E.A., 1993. Near-edge x-ray-absorption
637 fine-structure of pb - a comparison of theory and experiment. Phys Rev B 47, 14126-14131.

638 Nies, D.H., 1999. Microbial heavy-metal resistance. Appl Microbiol Biot 51, 730-750.

639 Norrod, E.P., Browne, S.L., Feldweg, A., Leonard, J., 1993. A dominant sulfhydryl-containing
640 protein in the outer-membrane of *neisseria-gonorrhoeae*. J Bacteriol 175, 1173-1175.

641 Petry, S., Furlan, S., Crepeau, M.J., Cerning, J., Desmazeaud, M., 2000. Factors affecting
642 exocellular polysaccharide production by *lactobacillus delbrueckii* subsp *bulgaricus* grown in a
643 chemically defined medium. Appl Environ Microb 66, 3427-3431.

644 Pokrovsky, O.S., Pokrovski, G.S., Shirokova, L.S., Gonzalez, A.G., Emnova, E.E., Feurtet-Mazel,
645 A., 2012. Chemical and structural status of copper associated with oxygenic and anoxygenic
646 phototrophs and heterotrophs: Possible evolutionary consequences. Geobiology 10, 130-149.

647 Ravel, B., Newville, M., 2005. Athena, artemis, hephaestus: Data analysis for x-ray absorption
648 spectroscopy using ifeffit. J Synchrotron Radiat 12, 537-541.

649 Rubino, F.M., 2015. Toxicity of glutathione-binding metals: A review of targets and mechanisms.
650 Toxics 3, 20-62.

651 Segre, C.U., Leyarovska, N.E., Chapman, L.D., Lavender, W.M., Plag, P.W., King, A.S., Kropf,
652 A.J., Bunker, B.A., Kemner, K.M., Dutta, P., Duran, R.S., Kaduk, J., 2000. The mrcat insertion
653 device beamline at the advanced photon source. Aip Conf Proc 521, 419-422.

654 Shamim, S., 2018. *Pseudomonas putida* mt2; a potential candidate for cadmium bioremediation.
655 Adv Sci Technol Inn 313-317.

656 Shamim, S., Rehman, A., Qazi, M.H., 2014. Cadmium-resistance mechanism in the bacteria
657 *cupriavidus metallidurans* ch34 and *pseudomonas putida* mt2. Arch Environ Con Tox 67, 149-
658 157.

659 Sheng, L., Fein, J.B., 2014. Uranium reduction by *shewanella oneidensis* mr-1 as a function of
660 nahco3 concentration: Surface complexation control of reduction kinetics. Environmental Science
661 & Technology 48, 3768-3775.

662 Shou, W.J., Kang, F.X., Lu, J.H., 2018. Nature and value of freely dissolved eps ecosystem
663 services: Insight into molecular coupling mechanisms for regulating metal toxicity. Environmental
664 Science & Technology 52, 457-466.

665 Stern, E.A., Heald, S.M., 1983. Basic principles and applications of exafs. Handbook of
666 Synchrotron Radiation 995-1014.

667 Stern, E.A., Newville, M., Ravel, B., Yacoby, Y., Haskel, D., 1995. The uwxafs analysis package
668 - philosophy and details. Physica B 208, 117-120.

669 Sunda, W.G., Engel, D.W., Thuotte, R.M., 1978. Effect of chemical speciation on toxicity of
670 cadmium to grass shrimp, palaemonetes-pugio - importance of free cadmium ion. Environmental
671 Science & Technology 12, 409-413.

672 Turner, R.J., 2017. Metal-based antimicrobial strategies. Microb Biotechnol 10, 1062-1065.

673 Wadhvani, S.A., Shedbalkar, U.U., Singh, R., Chopade, B.A., 2016. Biogenic selenium
674 nanoparticles: Current status and future prospects. Appl Microbiol Biot 100, 2555-2566.

675 Westall, J.C., Fiteql, a computer program for determination of chemical equilibrium constants
676 from experimental data. Version 2.0. Report 82-02, Dept. Chem., Oregon St. Univ., Corvallis, OR,
677 USA., 1982.

678 Yu, Q., Fein, J.B., 2015. The effect of metal loading on cd adsorption onto *shewanella oneidensis*
679 bacterial cell envelopes: The role of sulfhydryl sites. *Geochim Cosmochim Ac* 167, 1-10.

680 Yu, Q., Fein, J.B., 2016. Sulfhydryl binding sites within bacterial extracellular polymeric
681 substances. *Environmental Science & Technology* 50, 5498-5505.

682 Yu, Q., Fein, J.B., 2017a. Controls on bacterial cell envelope sulfhydryl site concentrations: The
683 effect of glucose concentration during growth. *Environmental Science & Technology* 51, 7395-
684 7402.

685 Yu, Q., Fein, J.B., 2017b. Enhanced removal of dissolved Hg(II), Cd(II), and Au(III) from water
686 by *bacillus subtilis* bacterial biomass containing an elevated concentration of sulfhydryl sites.
687 *Environmental Science & Technology* 51, 14360-14367.

688 Yu, Q., Szymanowski, J., Myneni, S.C.B., Fein, J.B., 2014. Characterization of sulfhydryl sites
689 within bacterial cell envelopes using selective site-blocking and potentiometric titrations. *Chem*
690 *Geol* 373, 50-58.

691

692